Korean J. Chem. Eng., **30**(12), 2151-2162 (2013)
DOI: 10.1007/s11814-013-0153-1

pISSN: 0256-1115
eISSN: 1975-7220

Analytical design of proportional-integral controllers for the optimal control of first-order processes with operational constraints

Hien Cao Thi Thu and Moonyong Lee†

School of Chemical Engineering, Yeungnam University, Gyeongsan 712-749, Korea
(*Received 8 March 2013 • accepted 7 August 2013*)

Abstract−A novel analytical design method of industrial proportional-integral (PI) controllers was developed for the optimal control of first-order processes with operational constraints. The control objective was to minimize a weighted sum of the controlled variable error and the rate of change in the manipulated variable under the maximum allowable limits in the controlled variable, manipulated variable and the rate of change in the manipulated variable. The constrained optimal servo control problem was converted to an unconstrained optimization to obtain an analytical tuning formula. A practical shortcut procedure for obtaining optimal PI parameters was provided based on graphical analysis of global optimality. The proposed PI controller was found to guarantee global optimum and deal explicitly with the three important operational constraints.

Key words: Analytical Design Rules, Constrained Optimization, First Order Process, Optimal Servo Control, Proportional-integral (PI) Controller, Controller Tuning, Smith Predictor

INTRODUCTION

In many industrial systems, such as two stirred tank reactors coupled by heat transfer [1], level control system [2] or absorption towers using swirling gas flow [3], optimal servo control has a direct impact on the accuracy and performance of the system. Precise servo control also holds the key to success in pneumatic robot systems [4], vibration isolation systems [5] and many other control products. In most optimal control cases, the control objective considers the variations not only in the controlled variable but also in the manipulated variable to cope with the performance and robustness together. Furthermore, many industrial control loops have several important constraints associated with both controlled and manipulated variables. This feature of an industrial control loop often requires an optimal control strategy with constraint handling.

Optimal control, as comprehensive meaning, deals with the problem of finding a control law for a given system such that a certain optimality criterion is achieved. Optimal control of a process with multiple constraints is quite challenging, even for a process with simple dynamics. Despite its usefulness, the constrained optimal control strategy has rarely been employed in industrial control loops that mainly use simple PI controllers, possibly because a PI controller is accepted as being too simple to implement any sophisticated control strategy. An analytical form of the optimal design method is attractive, but the complexity of the optimal control problem makes it unsuitable, even for very simple dynamic processes. The most typical and representative approach for optimal controller design is to use a classical optimal control framework derived using Pontryagin's principle or solving the Hamilton-Jacobi-Bellman equation [6-10] where the optimal PI parameters can be usually obtained by solving non-linear constrained optimization directly. Unfortunately, no numerical technique for non-linear optimization guarantees global optimal solution. For more complex nonlinear optimization problems, the stochastic optimization methods such as genetic algorithm (GA) [11,12], particle swarm optimization (PSO) [13,14], and heuristic Kalman algorithm (HKA) [15] can be applied. However, those computational approaches mainly use experimentation, evaluation and trial-and-error to obtain a numerical solution, and hardly provide truthful insights about the relations among process parameters as well as their effects on the constraints and optimal solutions [16]. Furthermore, many practitioners are unfamiliar with the use of complicated optimization packages.

To overcome these problems in finding optimal PI controller parameters, an optimization based approach for the analytical design was first developed for simple integrating processes for a regulatory problem with different types of constraint sets [17-20], and for a servo problem with multiple constraints [21]. This study extends the optimization-based approach for analytical design to general first-order processes, which is the representative dynamics of the majority process in the process industry. By focusing on minimizing a weighted sum of a controlled variable error and the rate of change in a manipulated variable, the proposed controller was also designed to satisfy the given maximum allowable limits in the output variable, manipulated variable and the rate of change in the manipulated variable. The constrained optimal servo control problem was first formulated and then converted to an equivalent unconstrained optimization in terms of two new independent variables by applying the Lagrange multiplier method. The optimal PI tuning rule was finally obtained from rigorous graphical analysis of possible cases with respect to the location of the global optimum. The resulting PI controller greatly improved the control performance by guaranteeing a global optimal solution while explicitly handling the important operational constraints. Another advantage of the proposed analytical design method is that it provides useful insights into the opti-

†To whom correspondence should be addressed.
E-mail: mynlee@yu.ac.kr

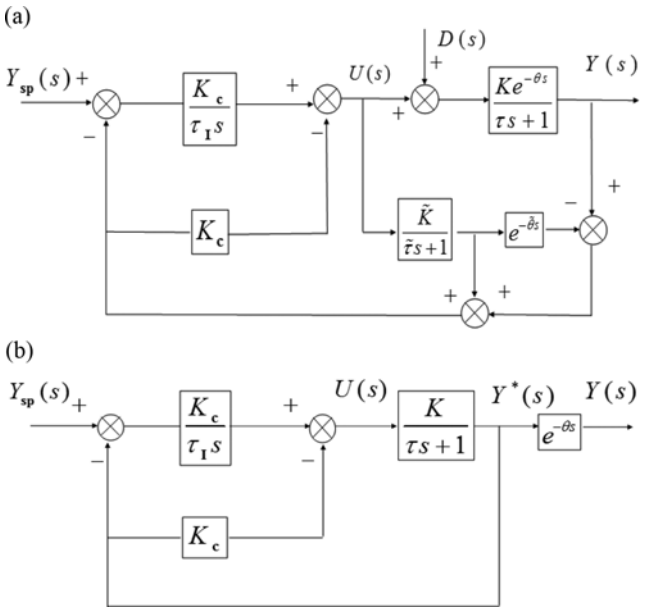

Fig. 1. (a) Block diagram of the feedback control of the FOPDT process with modified PI controller design and a conventional Smith predictor. (b) Block diagram of the feedback control of the proposed structure in the nominal case for the servo problem.

mal control behavior and its physical interpretation, which is impossible in any black box approach based on the direct application of non-linear optimization. The proposed design method was based on delay-free first-order processes. This method can also be applied directly to the delayed first-order processes by simply employing the Smith predictor structure.

DESIGN AND METHODOLOGY

1. Control System Description

Throughout this study, we assumed that the Smith predictor system as shown in Fig. 1(a) will be considered for a first-order process with a time delay, whereas a conventional feedback system was applied for a delay free first-order process. If there is no model-plant mismatch, the Smith predictor system can be expressed equivalently in a simpler configuration for the servo problem as in Fig. 1(b), where the time delay factor is eliminated from the feedback loop. Therefore, the controller can be designed based only on the delay free part of the process. A conventional feedback control system for a delay free first-order process is equivalent to the structure in Fig. 1(b) but the time delay block is removed: Y*(s)=Y(s). To avoid the proportional kick in the servo control, a modified PI controller, such as the PID controller with the type-C equation used in the Honeywell TDC™ system, was used.

The design problem then focused on finding the optimal PI controller parameters for a delay free first-order process. The effects of the set-point change on the outer and inner loops for the delay free process were then obtained as

$$Y^*(s)=\frac{1}{\varepsilon\tau_c\tau_I s^2+\varepsilon\tau_I s+1}Y_{sp}(s) \tag{1}$$

$$U(s)=\frac{\varepsilon K_c\frac{\tau_c}{\tau}(\tau s+1)}{\varepsilon\tau_c\tau_I s^2+\varepsilon\tau_I s+1}Y_{sp}(s) \tag{2}$$

where

$$\tau_c=\frac{\tau}{(1+KK_c)} \tag{3-1}$$

$$\varepsilon=\frac{1}{\left(1-\frac{\tau_c}{\tau}\right)} \tag{3-2}$$

The damping factor of the closed-loop transfer function above can be expressed as follows:

$$\zeta=\frac{1}{2}\sqrt{\frac{\varepsilon\tau_I}{\tau_c}}=\frac{1}{2}\sqrt{\frac{\tau}{(\tau-\tau_c)}\frac{\tau_I}{\tau_c}} \tag{3-3}$$

2. Formulation of Constrained Optimal Servo Control

In this study, the control objective of the optimal servo control was to minimize the weighted sum of the controlled variable error, e(t), and the rate of change in the manipulated variable, u′(t) , for a given set-point step change, Δy_{sp}, operating under the following three typical constraints:

(1) maximum allowable limit in the controlled variable, y_{max};

(2) maximum allowable limit in the rate of change in the manipulated variable, u'_{max}; (3) maximum allowable limit in the manipulated variable, u_{max}.

Therefore, the objective function can be defined by finding the controller parameters that minimize the performance measure in Eq. (4-1) for $\Delta y_{sp}/s$, subject to the constraints in Eqs. (4-2), (4-3) and (4-4):

$$\min \Phi=\omega_y\int_0^\infty (e(t))^2dt+\omega_u\int_0^\infty (u'(t))^2dt \tag{4-1}$$

subject to

$$|y(t)|\le y_{max} \tag{4-2}$$

$$|u'(t)|\le u'_{max} \tag{4-3}$$

$$|u(t)|\le u_{max} \tag{4-4}$$

where

$$e(t)=y(t)-y_{sp}(t) \tag{4-5}$$

Determining the optimal PI controller parameters by solving the non-linear optimization directly is still quite challenging and tedious. Furthermore, there is no guarantee of a global optimal solution. On the other hand, through clever parameterization, the above constrained optimization problems can be converted to a relatively simple algebraic form, which allows an analytical optimal solution as well as a graphical interpretation for its global optimality. Note that in the servo control of the Smith predictor system, minimizing $(y(t)-y_{sp}(t))^2$ is equivalent to minimizing $(y^*(t)-y_{sp}(t))^2$. Therefore, all derivations for the analytical solution will be based on the delay-free part. Through some mathematical manipulations, the above optimal control problem can be converted to the following algebraic problem expressed in term of two parameters, τ_c and ζ, as follows in Eqs. (5-1), (5-2), (5-3) and (5-4) (Derivation details are given in the Appendix):

$$\min \Phi(\tau_c, \zeta) = \alpha\tau_c(1+4\zeta^2) + \beta\frac{1}{\zeta^4\tau_c^3}\left(1+\frac{4\zeta^2\tau_c^2}{\tau^2}\right) \quad (5\text{-}1)$$

subject to

$$\gamma_g \geq g(\zeta) \quad (5\text{-}2)$$

$$\tau_c^2 \geq \gamma_h h(\zeta) \quad (5\text{-}3)$$

$$\tau_c \geq \gamma_f f(\tau_c, \zeta) \quad (5\text{-}4)$$

where

$$\alpha = \frac{\omega_y}{2}(\Delta y_{sp})^2;\ \beta = \frac{\omega_u}{32}\left(\frac{\tau}{K}\Delta y_{sp}\right)^2;$$

$$\gamma_g = \frac{y_{max}}{\Delta y_{sp}};\ \gamma_h = \left|\frac{\tau}{K}\frac{\Delta y_{sp}}{u'_{max}}\right|;\ \gamma_f = \left|\frac{\tau}{K}\frac{\Delta y_{sp}}{u_{max}}\right| \quad (6)$$

and $g(\zeta)$, $h(\zeta)$ and $f(\zeta)$ are given in Eqs. (A10), (A21) and (A16) in the Appendix, respectively.

Constraints given in Eqs. (5-2), (5-3) and (5-4) show that all three constraints are expressed in terms of τ_c and ζ, which allows the optimum location to be determined by graphical analysis of the three constraints and the contour of objective function in the (ζ, τ_c) space without the assistance of an optimization package.

3. Controller Design for Constrained Optimal Servo Control

Applying the Lagrangian multiplier [22] with slack variables converts the constrained optimization problem in Eqs. (5-1), (5-2), (5-3) and (5-4) to an unconstrained equivalent problem with an augmented objective function, as follows:

$$\min L(\tau_c, \zeta, \varpi_1, \varpi_2, \varpi_3, \sigma_1, \sigma_2, \sigma_3)$$

$$= \alpha\tau_c(1+4\zeta^2) + \beta\frac{1}{\tau_c^3\zeta^4}\left(1+\frac{4\zeta^2\tau_c^2}{\tau^2}\right) + \varpi_1(\tau_c^2 - \gamma_h h(\zeta) - \sigma_1^2) + \varpi_2(\gamma_g - g(\zeta) - \sigma_2^2) + \varpi_3(\tau_c - \gamma_f f(\zeta, \tau_c) - \sigma_3^2) \quad (7)$$

where, ϖ_i is the Lagrange multiplier ($\varpi_i \leq 0$), and σ_i is the slack variable.

The conditions necessary for an optimum solution are

$$\frac{\partial L}{\partial \tau_c} = \alpha(1+4\zeta^2) - \frac{3\beta}{\tau_c^4\zeta^4}\left(1+\frac{4\tau_c^2\zeta^2}{3\tau^2}\right) + 2\varpi_1\tau_c + \varpi_3(1-\gamma_f f'_{\tau_c}(\tau_c, \zeta)) = 0 \quad (8)$$

$$\frac{\partial L}{\partial \zeta} = 8\alpha\tau_c\zeta - \frac{4\beta}{\tau_c^3\zeta^5}\left(1+\frac{2\tau_c^2\zeta^2}{\tau^2}\right) - \varpi_1\gamma_h h'(\zeta) - \varpi_2 g'(\zeta) - \varpi_3\gamma_f f'_{\zeta}(\tau_c, \zeta) = 0 \quad (9)$$

$$\frac{\partial L}{\partial \varpi_1} = \tau_c^2 - \gamma_h h(\zeta) - \sigma_1^2 = 0 \quad (10)$$

$$\frac{\partial L}{\partial \varpi_2} = \gamma_g - g(\zeta) - \sigma_2^2 = 0 \quad (11)$$

$$\frac{\partial L}{\partial \varpi_3} = \tau_c - \gamma_f f(\tau_c, \zeta) - \sigma_3^2 = 0 \quad (12)$$

$$\frac{\partial L}{\partial \sigma_1} = -2\varpi_1\sigma_1 = 0;\ \frac{\partial L}{\partial \sigma_2} = -2\varpi_2\sigma_2 = 0;\ \frac{\partial L}{\partial \sigma_3} = -2\varpi_3\sigma_3 = 0 \quad (13)$$

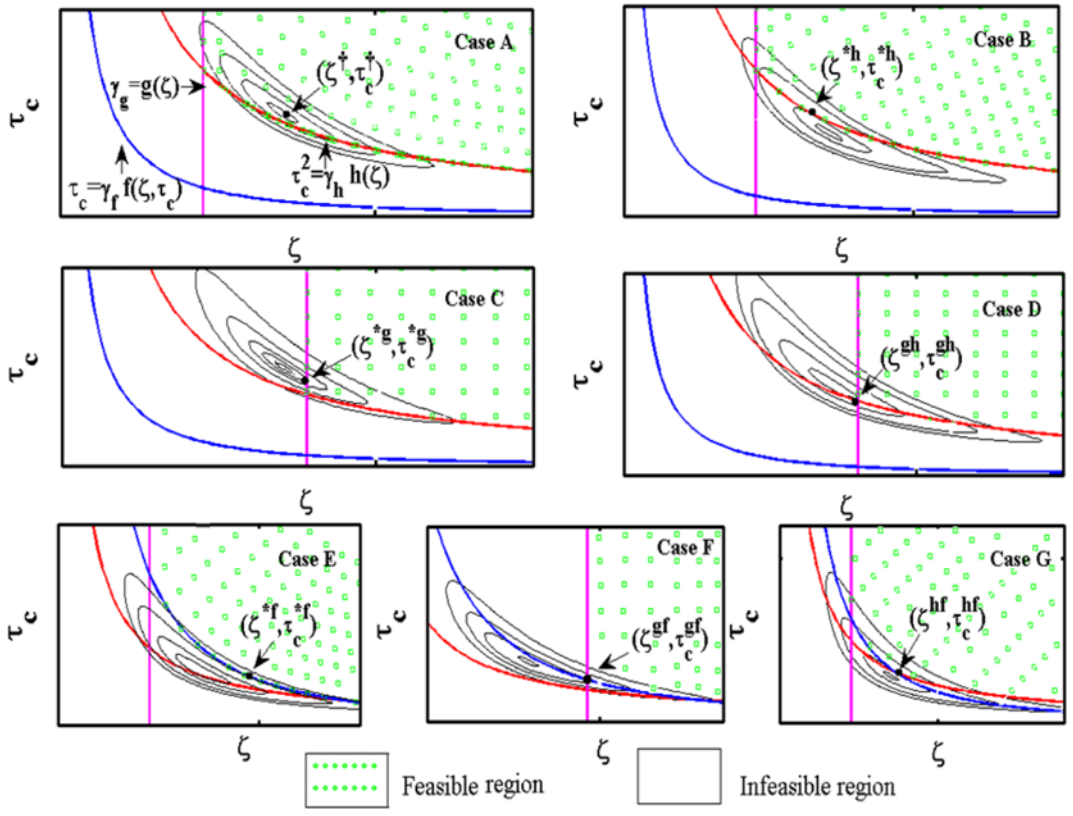

Fig. 2. Typical contours and constraints for the seven possible cases with respect to the global optimum location.

The simultaneous solutions in Eqs. (8), (9), (10), (11). (12) and (13) for various combinations of ϖ_i=0, ϖ_i≠0 and σ_i≠0 are associated with the corresponding optimum cases. Fig. 2 shows seven possible instances with respect to the location of the global optimum for the optimization problem in Eqs. (5-1) and (5-2). The global optimum can be located in the interior of the feasible region created by the three constraints (case A) on the boundary of one constraint (cases C, B, and E) or on the vertex formed by two constraints (cases D, F, and G).

The conditions associated with these seven cases can be evaluated by examining the geometrical characteristics of the contours and constraints in (ζ, τ_c) space. Finally, the global optimum of (ζ, τ_c) for each possible case is evaluated as follows:

Case A ($\varpi_1=\varpi_2=\varpi_3=0$): The extreme point, ($\zeta^{\dagger}$, $\tau_c^{\dagger}$), which is interior of the feasible region, becomes the global optimum.

The global optimum can be obtained by solving Eqs. (8) and (9) simultaneously:

$$\zeta^{\dagger}=\left(\frac{1}{2}+\frac{1}{\tau^2}\left(\frac{\beta}{\alpha}\right)^{\frac{1}{2}}\right)^{\frac{1}{2}} \tag{14-1}$$

and

$$\tau_c^{\dagger}=\left(\frac{\beta}{\alpha}\right)^{\frac{1}{4}}\frac{1}{\zeta^{\dagger}} \tag{14-2}$$

Case B ($\sigma_1=\varpi_2=\varpi_3=0$): The global optimum, which is denoted by (ζ^{*h}, τ_c^{*h}), is located on the constraint, $\tau_c^2=\gamma_h \mathrm{h}(\zeta)$.

ζ^{*h} can be calculated by replacing τ_c^{*h} with $\sqrt{\gamma_h \mathrm{h}(\zeta)}$ and substituting it to Eqs. (8) and (9)

$$\zeta^{*h}=\left(\frac{4\beta}{\alpha\gamma_h^2}+\frac{4\beta}{\tau^2\alpha\gamma_h}+\frac{1}{4}\right)^{\frac{1}{2}} \tag{15}$$

Inserting ζ^{*h} in Eq. (10), τ_c^{*h} can then be obtained as follows:

$$\tau_c^{*h}=(\gamma_h \mathrm{h}(\zeta^{*h}))^{\frac{1}{2}} \tag{16}$$

Case C ($\varpi_1=\sigma_2=\varpi_3=0$): The global optimum, which is denoted by (ζ^{*g}, τ_c^{*g}), is on the constraint $\mathrm{g}(\zeta)=\gamma_g$. ζ^{*g} is equivalent to the minimum allowable damping factor, ζ_{min}, which is calculated from Eq. (11).

τ_c^{*g} is then obtained by substituting ζ^{*g} into Eq. (8) as

$$\tau_c^{*g}=\left(\frac{3\beta}{\alpha(1+4\zeta_{min}^2)\zeta_{min}^4}\right)^{\frac{1}{4}}\left(\frac{2}{\tau}\left(\frac{\beta}{3\alpha\zeta_{min}}\right)^{\frac{1}{2}}+\left(\frac{4\beta}{3\tau(1+4\zeta_{min}^2)^4}+1\right)^{\frac{1}{2}}\right)^{\frac{1}{2}} \tag{17}$$

Case D ($\sigma_1=\sigma_2=\varpi_3=0$): The global optimum denoted by (ζ^{gh}, τ_c^{gh}) is located on the vertex point formed by $\tau_c^2=\gamma_h \mathrm{h}(\zeta)$ and $\mathrm{g}(\zeta)=\gamma_g$.

ζ^{gh} is also equivalent to ζ_{min}. τ_c^{gh} is calculated by substituting ζ^{gh} into Eq. (10) as

$$\tau_c^{gh}=(\gamma_h \mathrm{h}(\zeta_{min}))^{\frac{1}{2}} \tag{18}$$

Case E ($\varpi_1=\varpi_2=\sigma_3=0$): The global optimum, which is denoted as (ζ^{*f}, τ_c^{*f}) is on the constraint $\tau_c=\gamma_f \mathrm{f}(\tau_c, \zeta)$.

The optimal ζ^{*f} and τ_c^{*f} can be obtained by substituting Eq. (12) into Eqs. (8) and (9) and solving them simultaneously

$$\tau_c^{*f}-\gamma_f \mathrm{f}(\tau_c^{*f}, \zeta^{*f})=0 \tag{19}$$

$$\gamma_f \mathrm{f}_{\zeta}'(\zeta^{*f}, \tau_c^{*f})\left(\alpha(1+4(\zeta^{*f})^2)-\frac{3\beta}{(\zeta^{*f}\tau_c^{*f})^4}\left(1+\frac{4(\zeta^{*f}\tau_c^{*f})^2}{3\tau^2}\right)\right)$$
$$+(1-\gamma_f \mathrm{f}_{\tau_c}'(\zeta^{*f}, \tau_c^{*f}))\left(8\alpha\tau_c^{*f}\zeta^{*f}-\frac{4\beta}{(\zeta^{*f})^5(\tau_c^{*f})^3}\left(1+\frac{2(\zeta^{*f}\tau_c^{*f})^2}{\tau^2}\right)\right)=0 \tag{20}$$

where f_{ζ}' denotes the derivative of $\mathrm{f}(\zeta, \tau_c)$ in term of ζ, and f_{τ_c}' denotes the derivative of $\mathrm{f}(\zeta, \tau_c)$ in term of τ_c.

Case F ($\varpi_1=\sigma_2=\sigma_3=0$): The global optimum, which is denoted by (ζ^{gf}, τ_c^{fg}), is located on the vertex point formed by $\tau_c=\gamma_f \mathrm{f}(\tau_c, \zeta)$ and $\mathrm{g}(\zeta)=\gamma_g$.

ζ^{gf} is equivalent to ζ_{min}. τ_c^{fg} is then calculated by replacing ζ^{gf} with ζ_{min} and substituting it into Eq. (12) as

$$\tau_c^{gf}-\gamma_f \mathrm{f}(\tau_c^{gf}, \zeta_{min})=0 \tag{21}$$

Case G ($\sigma_1=\varpi_2=\sigma_3=0$): The global optimum, which is denoted by (ζ^{hf}, τ_c^{hf}), is located on the vertex point formed by $\tau_c=\gamma_f \mathrm{f}(\tau_c, \zeta)$ and $\tau_c^2=\gamma_h \mathrm{h}(\zeta)$.

ζ^{h} and τ_c^{hf} can be calculated by solving Eqs. (10) and (12) simultaneously

$$\tau_c^{hf}-\gamma_f \mathrm{f}(\tau_c^{hf}, \zeta^{hf})=0;\quad \tau_c^{hf}=(\gamma_h \mathrm{h}(\zeta^{hf}))^{\frac{1}{2}} \tag{22}$$

Once the global optimum is obtained in terms of ζ and τ_c, the corresponding optimal PI parameters can be calculated directly using Eqs. (3-1) and (3-2), which leads to

$$\mathrm{K}_c=\frac{\tau}{\mathrm{K}}\frac{\varepsilon^{opt}}{\tau_c^{opt}};\quad \tau_I=4(\zeta^{opt})^2\frac{\tau_c^{opt}}{\varepsilon^{opt}} \tag{23-1}$$

where

$$\varepsilon^{opt}=\frac{1}{\left(1-\frac{\tau_c^{opt}}{\tau}\right)} \tag{23-2}$$

Based on rigorous analysis of the geometrical characteristics of the contours and constraints, the conditions associated with the global optimum location were evaluated and are summarized in Table 1. The PI controller designed by the proposed method gives the optimal responses strictly satisfying all three given constraint specifications. The overall procedure for finding the global optimum quickly is also presented in Fig. 3.

4. Constraint Set and Feasible Region

In a constrained optimization problem, the global optimum can exist either on the extreme point or on the active constraints. Therefore, the feasibility of the solution region should be first checked for a given constraint set before being applied to a global optimal solution. Eqs. (A7), (A13) and (A19) in the Appendix show that the feasible values for y_{max} and u_{max} constraints must be not less than $|\Delta y_{sp}|$ and $|\Delta y_{sp}/\mathrm{K}|$, respectively, whereas any positive value is valid for u'_{max}. Fig. 4 shows the effect of three constraints specifications on the constraints and feasible region. The constraints imposed by Eq. (5-2) lay a vertical line, whereas the constraints given in Eqs.

Table 1. Global optimal of the constrained optimization problem in Eqs. (5-1), (5-2), (5-3) and (5-4)

Case	Lagrange parameter	Typical specification	Condition	Global optimum	Calculation of global optimum
A	$\varpi_1=\varpi_2=\omega_3=0$	Mild u'_{max} Mild y_{max} Mild u_{max}	$\zeta_{min}\le\zeta^{\dagger}$ and $\tau_c^{\dagger}\ge\max(\tau_c^{*h}, \tau_c^{*f})$	$(\zeta^{\dagger}, \tau_c^{\dagger})$ in the interior of the feasible region	$\zeta^{\dagger}=\left(\frac{1}{2}+\frac{1}{\tau^2}\left(\frac{\beta}{\alpha}\right)^{\frac{1}{2}}\right)^{\frac{1}{2}}$ $\tau_c^{\dagger}=\left(\frac{\beta}{\alpha}\right)^{\frac{1}{4}}\frac{1}{\zeta^{\dagger}}$
B	$\sigma_1=\varpi_2=\varpi_3=0$	Tight u'_{max} Mild y_{max} Mild u_{max}	$\tau_c^{\dagger}<\max(\tau_c^{*h}, \tau_c^{*f})$ and $\zeta^{*h}>\max(\zeta^{hf}, \zeta_{min})$	$(\zeta^{*h}, \tau_c^{*h})$ on $\tau_c^2=\gamma_h h(\zeta)$	$\zeta^{*h}=\left(\frac{4\beta}{\alpha\gamma_h^2}+\frac{4\beta}{\tau^2\alpha\gamma_h}+\frac{1}{4}\right)^{\frac{1}{2}}$ $\tau_c^{*h}=(\gamma_h h(\zeta^{*h}))^{\frac{1}{2}}$
C	$\sigma_2=\varpi_1=\varpi_3=0$	Mild u'_{max} Tight y_{max} Mild u_{max}	$\zeta_{min}>\zeta^{\dagger}$ and $\tau_c^{*g}>\max(\tau_c^{gh}, \tau_c^{gf})$	$(\zeta^{*g}, \tau_c^{*g})$ on $g(\zeta)=\gamma_g$	$g(\zeta^{*g})=\gamma_g$ $\tau_c^{*g}=F_1(\zeta^{*g})$
D	$\sigma_1=\sigma_2=\omega_3=0$	Tight u'_{max} Tight y_{max} Mild u_{max}	$[\tau_c^{\dagger}\ge\max(\tau_c^{*h}, \tau_c^{*f})$ and $\zeta_{min}>\zeta^{\dagger}$ and $\tau_c^{gh}>\max(\tau_c^{*g}, \tau_c^{gf})]$ or $[\tau_c^{\dagger}<\max(\tau_c^{*h}, \tau_c^{*f})$ and $\zeta^{gh}>\max(\zeta^{hf}, \zeta^{*h})]$	$(\zeta^{gh}, \tau_c^{gh})$ on the vertex by $g(\zeta)=\gamma_g$ and $\tau_c^2=\gamma_h h(\zeta)$	$g(\zeta^{gh})=\gamma_g$ $\tau_c^{gh}=(\gamma_h h(\zeta^{gh}))^{\frac{1}{2}}$
E	$\omega_1=\omega_2=\sigma_3=0$	Mild u'_{max} Mild y_{max} Tight u_{max}	$\tau_c^{\dagger}<\max(\tau_c^{*h}, \tau_c^{*f})$ and $\zeta_{min}<\zeta^{*f}<\zeta^{hf}$	$(\zeta^{*f}, \tau_c^{*f})$ on $\gamma_f=f(\tau_c, \zeta)$	$F_2(\zeta^{*f}, \tau_c^{*f})=0$ $\gamma_f=f(\zeta^{*f}, \tau_c^{*f})$
F	$\omega_1=\sigma_2=\sigma_3=0$	Mild u'_{max} Tight y_{max} Tight u_{max}	$[\tau_c^{\dagger}\ge\max(\tau_c^{*h}, \tau_c^{*f})$ and $\zeta_{min}>\zeta^{\dagger}$ and $\tau_c^{gf}>\max(\tau_c^{*g}, \tau_c^{gh})]$ or $[\tau_c^{\dagger}<\max(\tau_c^{*h}, \tau_c^{*f})$ and $\zeta^{*f}<\zeta_{min}<\zeta^{hf}]$	$(\zeta^{gf}, \tau_c^{gf})$ on the vertex by $g(\zeta)=\gamma_g$ and $\gamma_f=f(\tau_c, \zeta)$	$g(\zeta^{gf})=\gamma_g$ $\gamma_f=f(\zeta^{gf}, \tau_c^{gf}))$
G	$\omega_2=\sigma_1=\sigma_3=0$	Tight u'_{max} Mild y_{max} Tight u_{max}	$\tau_c^{\dagger}<\max(\tau_c^{*h}, \tau_c^{*f})$ and $\zeta_{min}<\zeta^{*h}<\zeta^{hf}$	$(\zeta^{gh}, \tau_c^{gh})$ on the vertex by $g(\zeta)=\gamma_g$ and $\gamma_f=f(\tau_c, \zeta)$	$\gamma_f=f(\zeta^{hf}, \tau_c^{hf})$ $\tau_c^{hf}=\frac{\sqrt{\gamma_h}}{2\zeta^{hf}}$

$$F_1(\zeta^{*g})=\left(\frac{3\beta}{\alpha(1+4(\zeta^{*g})^2)(\zeta^{*g})}\right)^{\frac{1}{4}}\left(\frac{2}{\tau}\left(\frac{\beta}{3\alpha\zeta^{*g}}\right)^{\frac{1}{2}}+\left(\frac{4\beta}{3\tau(1+4(\zeta^{*g})^2)^4}+1\right)^{\frac{1}{2}}\right)^{\frac{1}{2}}$$

$$F_2(\zeta^{*f}, \tau_c^{*f})=\gamma_f f'_{\zeta}(\zeta^{*f}, \tau_c^{*f})\left(\alpha(1+4(\zeta^{*f})^2)-\frac{3\beta}{(\zeta^{*f}\tau_c^{*f})^4}\left(1+\frac{4(\zeta^{*f}\tau_c^{*f})^2}{3\tau^2}\right)\right)$$
$$+(1-\gamma_f f'_{\tau_c}(\zeta^{*f}, \tau_c^{*f}))\left(8\alpha\tau_c^{*f}\zeta^{*f}-\frac{4\beta}{(\zeta^{*f})^5(\tau_c^{*f})^3}\left(1+\frac{2(\zeta^{*f}\tau_c^{*f})^2}{\tau^2}\right)\right)$$

(5-3) and (5-4) provide curves with a similar shape in (ζ, τ_c) space. As the y_{max}, u_{max} and u'_{max} specifications decrease, the feasible region surrounded by these constraints becomes narrow but is always available and unbounded with any feasible constraint set. Moreover, the feasible solution region is always convex from the shape of the three constraints. Note that as y_{max} decreases, approaching Δy_{sp}, the vertical line by the constraint, $\gamma_g=g(\zeta)$, moves to the right and eventually at $\zeta=1$ in (ζ, τ_c) space.

SIMULATION STUDY

Consider the following first-order plus time delay (FOPDT) process as

$$G_p(s)=\frac{10e^{-s}}{s+1} \tag{24}$$

The weighting factors were chosen arbitrarily as $\omega_y=\omega_u=0.5$. Examples of cases A-G with different constraint specifications were considered, and are listed in Table 2. Figs. 5 and 6 show the responses of the controlled variable, y(t), the rate of change in the manipulated variable u′(t) and the manipulated variable u(t) for the seven examples. As shown in the figures, the PI controller designed by the proposed method provides the optimal responses while strictly satisfying the y_{max}, u'_{max} and u_{max} constraints.

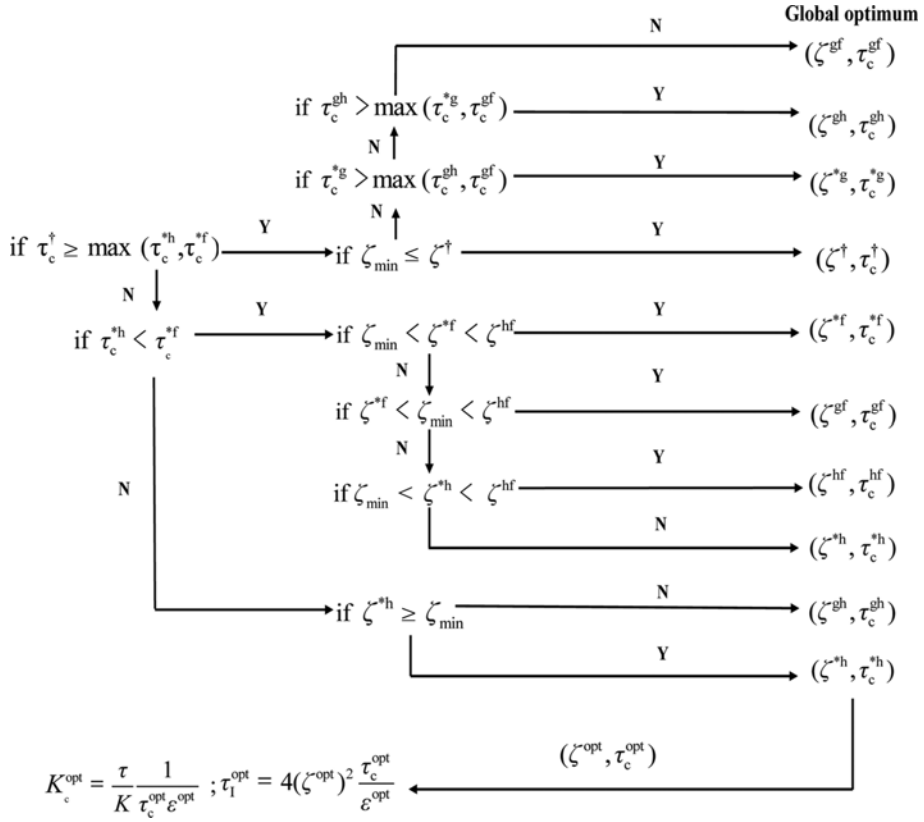

Fig. 3. Flow chart for finding the global optimum and corresponding PI parameters.

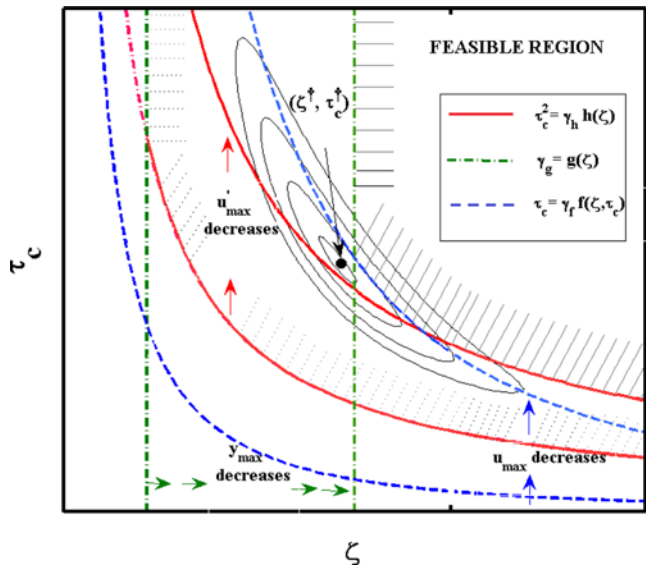

Fig. 4. Effect of the y_{max}, u'_{max} and u_{max} specifications on the constraints and feasible region.

To highlight the advantage of the proposed method, the closed-loop performance of the proposed PI controller was compared with that of the IMC-PI controller [23] under the same structure in Fig. 1 for example 1. The tuning parameter, λ, of the IMC-PI controller was adjusted for the following two cases:

(1) to give the minimum objective function value provided the responses of y(t), u(t) and u′(t) satisfy all the given constraints specifications (λ=0.45)

(2) to give the minimum objective function value without considering the constraint specifications (λ=0.301)

Fig. 7 presents the results of the comparison. Table 3 lists the performance matrix for the servo problem. The PI controller by the proposed method provided the smallest value of the objective function satisfying all three constraints. On the other hand, the PI controller designed by the IMC-PI method resulted in larger objective function values in both cases: the constraints were violated when it provided the smallest possible objective value; and a large value of the objective function with slow responses was provided when λ was adjusted to satisfy all the constraints. These results confirm the advan-

Table 2. Constraint specifications and resulting optimal PI parameters

Example	Case	Specifications			Optimal PI parameters	
		u'_{max}	y_{max}	u_{max}	K_c	τ_I
1	A	1.05	1.05	0.20	0.358	0.358
2	B	0.90	1.05	0.20	0.292	0.324
3	C	1.05	1.01	0.20	0.394	0.374
4	D	0.50	1.01	0.15	0.269	0.509
5	E	0.40	1.05	0.13	0.195	0.622
6	F	0.20	1.01	0.11	0.112	0.682
7	G	0.50	1.05	0.12	0.348	0.697

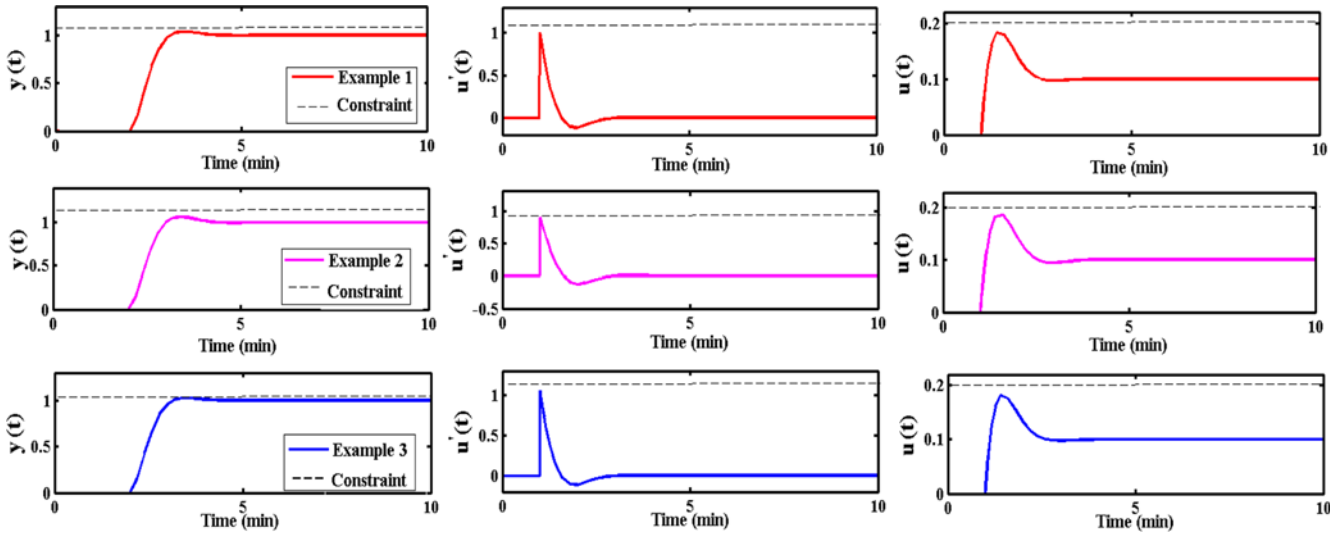

Fig. 5. Responses of y(t), u′(t) and u(t) for examples (1) to (3).

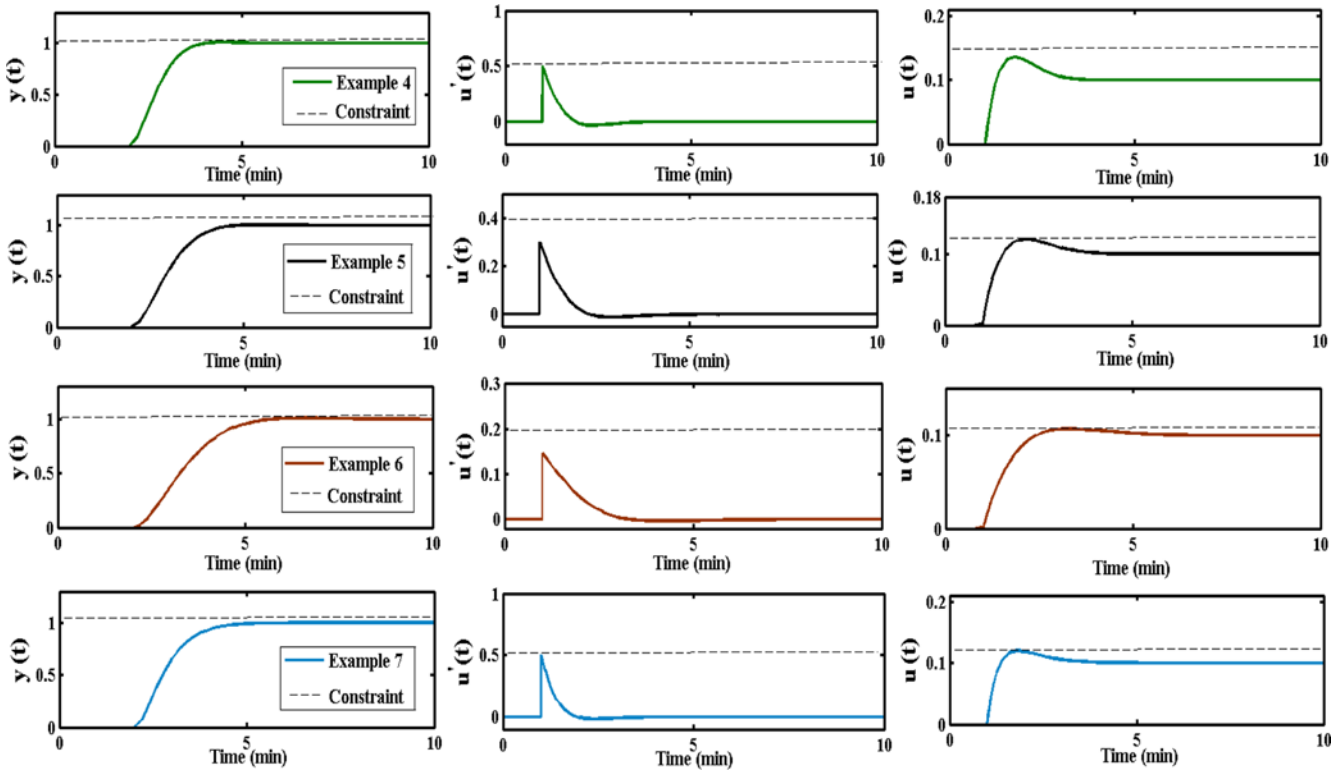

Fig. 6. Responses of y(t), u′(t) and u(t) for examples (4) to (7).

tages of the proposed method.

DISCUSSION

1. Effect of Weighting Factors

In the optimal control, the weighting factor, ω, is a crucial parameter to adjust the control performance and robustness. The weight of the controlled variable on the performance measure increased with increasing ω_y. Accordingly, the optimal PI controller yields a tighter control response. On the other hand, when a larger ω_u is chosen, the main control objective is not to control the controlled variable fast but rather smoothly. Fig. 8 shows how the global optimum and extreme point locations vary with the weighting factor when the constraints by the y_{max} and u'_{max} specifications are applied. When ω_y is set to a small value, such as ω_y=0.1 (or ω_u was set to a large value), the performance measure of the optimal control is determined mainly by the variation of the rate of change in the manipulated variable. Accordingly, the optimal controller provides a tight response of the rate of change in the manipulated variable and the response is constrained by the y_{max} specifications. Furthermore, because the extreme

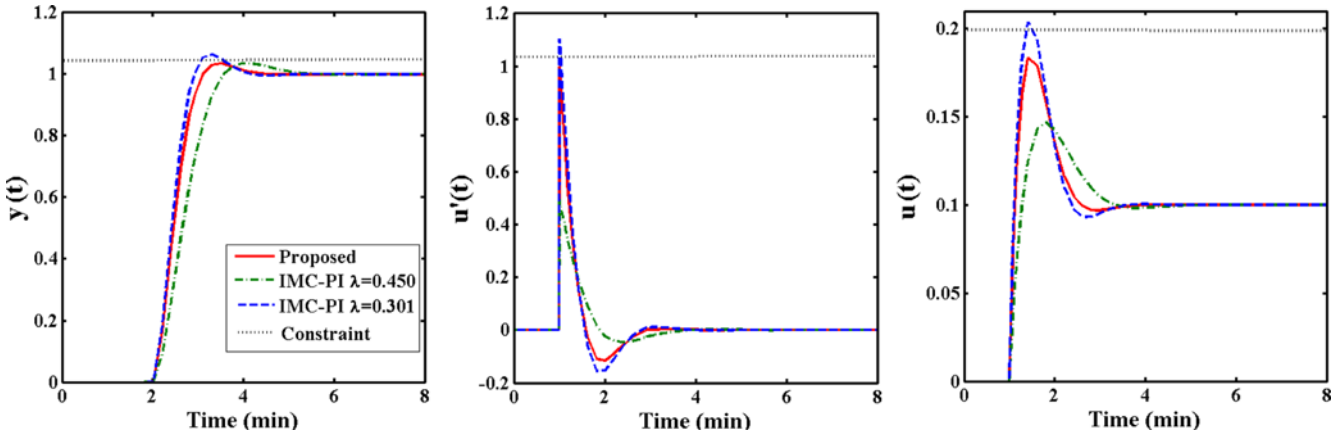

Fig. 7. Responses of y(t), u′(t) and u(t) using the proposed method and IMC-PI method.

Table 3. PI parameters and performance of the IMC-PI method and proposed method

Method	λ	Specifications			PI parameters		Objective function
		u'_{max}	y_{max}	u_{max}	K_c	τ_I	
Proposed	-	1.05	1.05	0.2	0.358	0.358	0.237
IMC-PI	0.450	1.05	1.05	0.2	0.222	0.450	0.266
	0.301	1.05	1.05	0.2	0.322	0.301	0.243

point is likely to be located above the boundary of $\tau_c^2=\gamma_h h(\zeta)$, the global optimal point will be either on the extreme point, i.e., case A or on $\gamma_g=g(\zeta)$, i.e., case C, as indicated in Fig. 8. When a larger ω_y bis applied, the performance measure of optimal control is determined mainly by the variation of the controlled variable, the optimal controller yields a tight response of the controlled variable, and the response is constrained by the u'_{max} specification. Moreover, the extreme point shifts the location to the left and lower direction in (ζ, τ_c) space, and the optimal solution is likely to occur on the constraint, $\tau_c^2=\gamma_h h(\zeta)$, formed by the u'_{max} specification, i.e., case B. Fig. 9 shows the responses of the controlled variable and the rate of change in the manipulated variable for various weighting factor settings when y_{max}=1.1 and u'_{max}=3. As observed from the figure, the optimal PI controller yields a tighter and faster control response as ω_y increases, whereas there is a smoother control response with a small rate of change in the manipulated variable when a larger ω_u

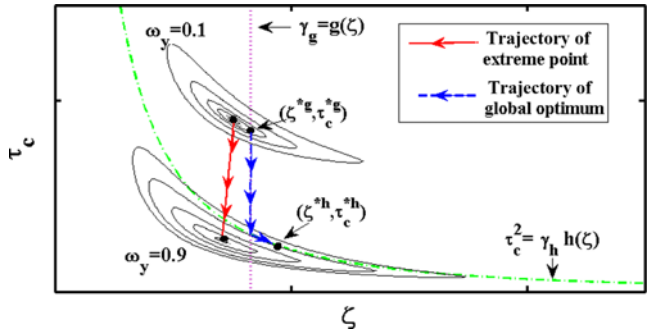

Fig. 8. Effect of the weighting factor on the trajectories of the extreme point and global optimum.

is chosen. Note that the proposed PI controller strictly satisfies the constraints by the y_{max} and u'_{max} specifications, regardless of the weighting factor setting.

Remark: For unconstrained case (case A), the ratio of the optimal proportional gain, K_c^{opt}, to the optimal integral time, τ_I^{opt}, is independent of the other process parameters and only a function of the weighting factor, in particular, equal to the square root of the ratio of ω_y to ω_u

$$\frac{K_c^{opt}}{\tau_I^{opt}}=\sqrt{\frac{\omega_y}{\omega_u}} \tag{25}$$

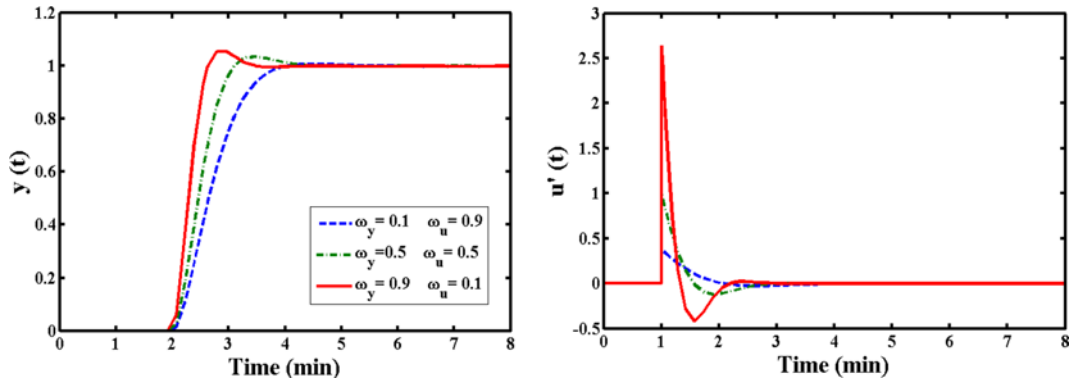

Fig. 9. Effect of the weighting factor on the responses of y(t) and u′(t).

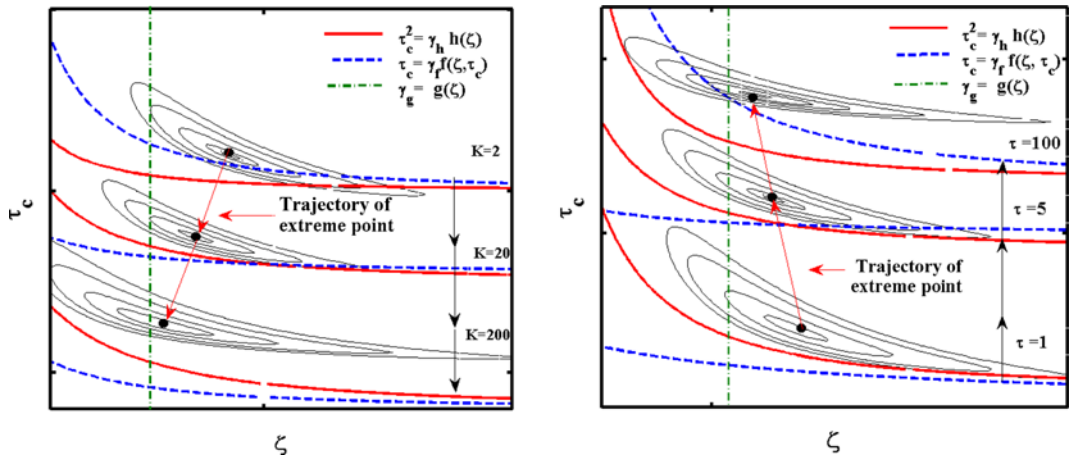

Fig. 10. Effect of the process parameters on the trajectories of the extreme point and global optimum.

Furthermore, the peak value of the rate of change in the manipulated variable for the unit step set-point is also equal to the square root of the ratio of ω_y to ω_u as

$$\frac{u'_{peak}}{\Delta y_{sp}} = \sqrt{\frac{\omega_y}{\omega_u}} \tag{26}$$

This explains the independence of u'_{peak} on the process parameters variations, as shown in Figs. 11 and 12.

3. Effect of the Process Parameters

The process parameters affect the shape and location of the constraints as well as the objective function contour in (ζ, τ_c) space, which results in different global optima in the control parameters and different behaviors of the optimal controller. Fig. 10 shows how the constraint curves, extreme point, and thus the global optimum, vary with the process gain and time constant. As the process gain, K, increases, the extreme point moves to a lower left position and the constraints by u'_{max} and u_{max} shift to a lower position in (ζ, τ_c) space. The constraint by u'_{max} also changes from lower to higher position than that by u_{max} simultaneously. The optimal response therefore is likely to be constrained by y_{max} or u'_{max} from u_{max} as K increases further. In contrast, as the time constant, τ, increases, the extreme point shifts to a higher left position and the two constraints a higher

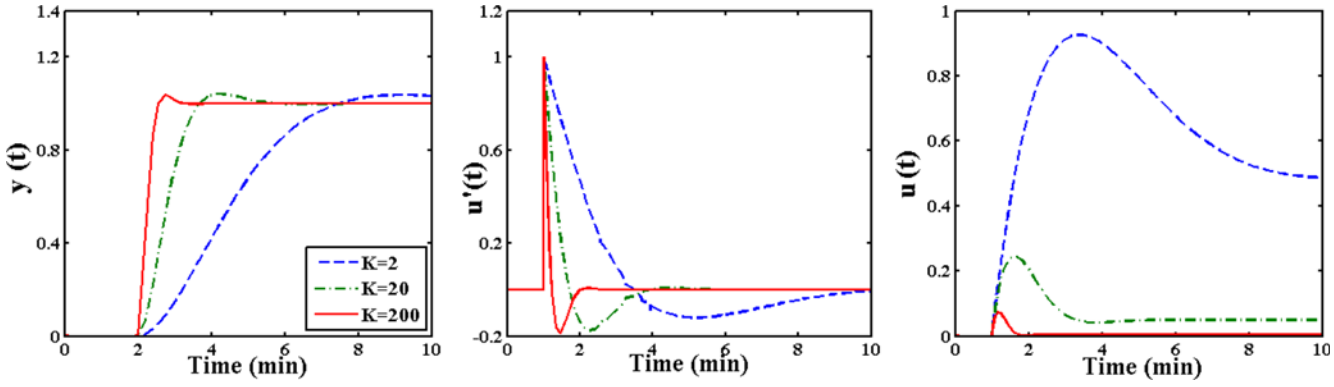

Fig. 11. Effect of the process gain on the responses of y(t), u′(t) and u(t).

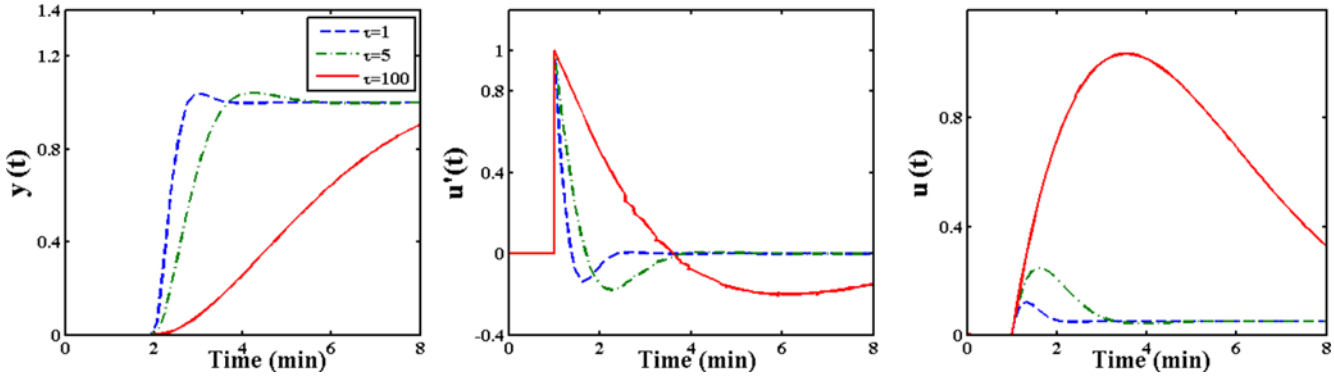

Fig. 12. Effect of the time constant on the responses of y(t), u′(t) and u(t).

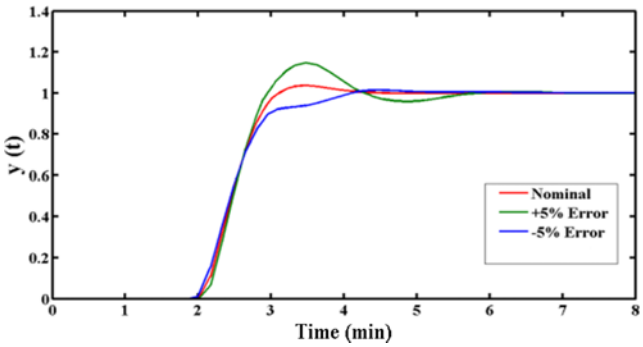

Fig. 13. Effect of plant-model mismatch.

position in (ζ, τ_c) space. In this case, the constraint by u'_{max} shifts from higher to lower position than that by u_{max} simultaneously. The optimal response therefore firstly is likely to be constrained by u'_{max} and then by y_{max} and u_{max} as τ increases further. Note that the constraint by y_{max} is independent of the process parameters.

Fig. 11 shows the closed loop responses for a range of values of the process gain, K, where a constraint set was chosen as y_{max}=1.05, u'_{max}=10, u_{max}=1.0, and the other parameters were fixed at τ=5, ω_y=ω_u=0.5. Fig. 12 presents the closed loop responses for various values of the time constant, τ, where the constraints of y_{max}=1.05, u'_{max}=10, u_{max}=1.0 were selected and K=20; ω_y=ω_u=0.5. Note that these two cases belong to case A. As observed in the responses, a larger K value results in faster responses of the optimal controller with a larger overshoot. On the other hand, a larger τ causes slower responses of the optimal controller with a smaller overshoot.

4. Robustness for Plant-Model Mismatch

Robustness is important to any controller design. The robustness of the proposed controller was evaluated by inserting a perturbation uncertainty of ±5% in all three process parameters simultaneously to obtain the model mismatch case for the sample process given in Eq. (24). The simulation result comparing the responses for nominal and model mismatch cases is shown in Fig. 13. The result indicates the control performance does not sensitively change the proposed controller against the uncertainty given. Note that this sensitivity is independent on the approach to get the optimal solution but implies how sensitively the control performance of the FOPDT process deviates from its global optimality for given parametric uncertainties.

CONCLUSIONS

Clever parameterization of an optimal control formulation allows an analytical tuning rule of the PI parameters for the optimal servo control of first-order processes with multiple operational constraints. The proposed design method explicitly deals with the representative type of constraints as well as minimizing the general cost function of optimal servo control problems. Rigorous graphical analysis of the contour and constraints showed that the possible optimal cases must belong to one of the seven cases, depending on the location of the optimal solution in (ζ, τ_c) space. The proposed simple analytical tuning procedure allows the optimal PI parameters to be found quickly and guarantees their globally optimality without the need for complex optimization packages, which often leads to a non-optimal solution and require many trials. The proposed method is based mainly on delay-free first-order processes but can be applied directly to time-delayed processes by simply employing the Smith predictor structure. The proposed controller yields the optimal servo responses strictly satisfying the three given constraint specifications. The analytical form for the controller design also gives control practitioners a useful insight into the effects of the process and design parameters on control performance.

ACKNOWLEDGEMENTS

This research was supported by a Yeungnam university grant in 2011.

NOMENCLATURE

D(s) : transfer function of the disturbance variable
e(t) : controlled variable error
K : plant process gain
K_c : proportional gain
$\tilde{K}$: model process gain
U(s) : transfer function of the manipulated variable
u(t) : time function of the manipulated variable
u_{max} : maximum allowable limit of the manipulated variable
u'_{max} : maximum allowable limit of the rate of change of the manipulated variable
u′(t) : time function of the rate of change of the manipulated variable
Y(s) : transfer function of the controlled variable
Y_{sp}(s) : transfer function of the set point variable
y(t) : time function of the controlled variable
y_{max} : maximum allowable limit of the controlled variable
Δy_{sp} : expected maximum step change in the set point
ζ : damping factor
σ_i : slack variable
θ : plant dead time [min]
$\tilde{\theta}$: model dead time [min]
τ : plant time constant [min]
τ_I : integral time constant [min]
$\tilde{\tau}$: model time constant [min]
ϖ_i : Lagrangian multiplier
ω_y, ω_u, ω : weighting factors

REFERENCES

1. J. C. Mankin and J. L. Hudson, *Chem. Eng. Sci.*, **41**, 2651 (1986).
2. R. Zhang, A. Xue and S. Wang, *Chem. Eng. Sci.*, **66**, 6002 (2001).
3. K. H. Javed and T. Mahmud, *Chem. Eng. Res. Des.*, **84**, 465 (2006).
4. M. Takashi, F. Toshinori, S. Kazutoshi, K. Kenji and K. Toshiharu, *Prec. Eng.*, **31**, 156 (2007).
5. H. Roberto, L. Yunfeng, O. Kenn, K. Stanley and H. Xinghui, *Con. Eng. Prac.*, **15**, 291 (2007).
6. F. L. Lewis, *Optimal control*, New York, John Wiley and Sons (1986).
7. A. M. Letov, *Automat Rem Contr.*, **21**, 4, 303 (1960).
8. L. S. Pontryagin, V. G. Boltyanskii, R. V. Gamkrelidze and E. F. Mis-

chenko, The 34 The Standard Regulator Problem—1 Chap. 2 Mathematical Theory of Optimal Processes, K. N. Trirogoff (transl.), L. W. Neustadted, Interscience, New York (1962).
9. C. D. Siebenthal and R. Aris, *Chem. Eng. Sci*., **19**, 10, 729 (1964).
10. A. P. Sage, Optimal Systems Control. Prentice-Hall, Inc., Englewood Cliffs, N. J. (1968).
11. X. P. Zeng, Y. M. Li and J. Qin, *Neurocomputing*, **72**, 4-6, 1241 (2009).
12. D. E. Goldberg, Genetic Algorithms in Search, *Optimization and machine learning*, Kluwer Academic Publishers, Boston, MA (1989).
13. F. van den Bergh and A. P. Engelbrecht, *Inform Sciences*, **176**, 937 (2006).
14. Q. He and L.Wang, *Eng. Appl. Artif. Intel*., **20**, 89 (2007).
15. R. Toscano and P. Lyonnet, *IEEE Systems, Man, and Cybernetics Society*, **39**, 5, 1231 (2009).
16. M. Kurt, *Stochastic optimization methods*, 2nd Ed, Springer (2008).
17. J. Shin, J. Lee, S. Park, K. Koo and M. Lee, *Con. Eng. Prac*., **16**, 1391 (2008).
18. M. Lee and J. Shin, *Chem. Eng. Commun*., **196**, 729 (2009).
19. M. Lee, J. Shin and J. Lee, *Hydrocarbon Processing*, **89**, 71 (2010).
20. M. Lee, J. Shin and J. Lee, *Hydrocarbon Processing*, **89**, 81 (2010).
21. V. H. Nguyen, Y. Yoshiyuki and M. Lee, *J. Chem. Eng. Jpn*., **44**, 345 (2011).
22. I. B. Vapnyarskii, *Lagrange multipliers*, In: Hazewinkel, M. (ed.). Encyclopedia of Mathematics, Springer, Heidelberg (2001).
23. D. E. Rivera, M. Morari and S. Skogestad, *Ind. Eng. Chem. Proc. Des. Dev*., **25**, 252 (1986).

APPENDICES

1. Appendix A. Derivation of the Performance Measure, ϕ, Given in Eq. (4-1)

Consider a delay free first-order process. For a step change in the set point of the controlled variable, i.e., $y_{sp}=\Delta y_{sp}/s$, e(t) and u′(t) given in Eqs. (1) and (2) are obtained as follows.

$$e(t)=\Delta y_{sp}\left(\frac{r_2e^{r_1t}-r_1e^{r_2t}}{r_1-r_2}\right) \quad \text{for } r_1\neq r_2 \tag{A1}$$

$$u'(t)=-\frac{K_c\Delta y_{sp}}{\tau_1}\left(\frac{-r_1e^{r_1t}+r_2e^{r_2t}+(-e^{r_1t}+e^{r_2t})\frac{1}{\tau}}{r_1-r_2}\right) \quad \text{for } r_1\neq r_2 \tag{A2}$$

where r_1 and r_2 are the roots of the characteristic equation, $\varepsilon\tau_c\tau_I s^2+\varepsilon\tau_I s+1=0$.

$$r_1=\frac{-1+xi}{2\tau_c};\quad r_2=\frac{-1-xi}{2\tau_c} \tag{A3}$$

and

$$\begin{aligned} x&=\frac{\sqrt{1-\zeta^2}}{\zeta} \quad \text{for } 0<\zeta\leq 1\\ &=\frac{\sqrt{\zeta^2-1}}{\zeta} \quad \text{for } \zeta>1\end{aligned} \tag{A4}$$

Note that this notation for x will be used throughout the Appendix. Therefore, the performance measure for optimal control was derived as

$$\begin{aligned}&\omega_y\int_0^\infty (e(t))^2dt+\omega_u\int_0^\infty (u'(t))^2dt\\ &=\omega_y(\Delta y_{sp})^2\left(\frac{1}{r_1-r_2}\right)^2\left(-\frac{r_1^2}{2r_2}-\frac{r_2^2}{2r_1}+\frac{2r_1r_2}{(r_1+r_2)}\right)\\ &+\omega_u\left(-\frac{K_c\Delta y_{sp}}{\tau_I}\right)^2\times\left(\frac{1}{r_1-r_2}\right)^2\left(-\frac{r_1}{2}-\frac{r_2}{2}+\frac{2r_1r_2}{(r_1+r_2)}\right)\\ &=\alpha\tau_c(1+4\zeta^2)+\beta\frac{1}{\tau_c^3\zeta^4}\left(1+\frac{4\zeta^2\tau_c^2}{\tau^2}\right)\end{aligned} \tag{A5}$$

2. Appendix B. Derivation of the Constraint Given in Eq. (4-2)

The response of the controlled variable to a step change in the set point was obtained from the inverse Laplace transform of the equation given in Eq. (1)

$$\begin{aligned} y(t)&=\Delta y_{sp}\left(1-\exp\left(-\frac{t}{2\tau_c}\right)\left(\cos\left(\frac{x}{2\tau_c}t\right)+\frac{1}{x}\sin\left(\frac{x}{2\tau_c}t\right)\right)\right) && \text{for } 0<\zeta<1\\ &=\Delta y_{sp}\left(1-\left(\frac{t}{2\tau_c}+1\right)\exp\left(-\frac{t}{2\tau_c}\right)\right) && \text{for } \zeta=1\\ &=\Delta y_{sp}\left(1-\exp\left(-\frac{t}{2\tau_c}\right)\left(\cosh\left(\frac{x}{2\tau_c}t\right)+\frac{1}{x}\sinh\left(\frac{x}{2\tau_c}t\right)\right)\right) && \text{for } \zeta>1\end{aligned} \tag{A6}$$

The steady-state response of the controlled variable to a step change in the set point is defined as t approaches infinity and was obtained as follows:

$$y_{ss}\ (t\rightarrow\infty)=\Delta y_{sp} \tag{A7}$$

From the differentiation of y(t), the peak time for the largest peak in the controlled variable was obtained as

$$\begin{aligned} t_{peak}&=\frac{2\tau_c\pi}{x} && \text{for } 0<\zeta<1\\ &=\infty && \text{for } \zeta\geq 1\end{aligned} \tag{A8}$$

The peak of y(t) was found as follows:

$$y_{peak}=\Delta y_{sp}\cdot g(\zeta) \tag{A9}$$

where

$$\begin{aligned} g(\zeta)&=1+\exp\left(-\frac{\pi}{x}\right) && \text{for } 0<\zeta<1\\ &=1 && \text{for } \zeta\geq 1\end{aligned} \tag{A10}$$

Therefore, the constraint in Eq. (4-2) can be expressed as

$$\Delta y_{sp}\cdot g(\zeta)\leq y_{max} \tag{A11}$$

3. Appendix C. Derivation of the Constraint Given in Eq. (4-4)

The response of the manipulated variable to a step change in the set point is obtained from the inverse Laplace transform of the equation given in Eq. (2):

$$\begin{aligned} u(t)&=\frac{\tau}{K}\frac{\Delta y_{sp}}{2\tau_c\zeta^2x}\left(\exp\left(-\frac{t}{2\tau_c}\right)\sin\left(\frac{x}{2\tau_c}t\right)-\frac{2\tau_c\zeta^2x}{\tau}\right.\\ &\left.\left(1-\exp\left(-\frac{t}{2\tau_c}\right)\left(\cos\left(\frac{x}{2\tau_c}t\right)+\frac{1}{x}\sin\left(\frac{x}{2\tau_c}t\right)\right)\right)\right) && \text{for } 0<\zeta<1\\ &=\frac{\tau}{K}\frac{\Delta y_{sp}}{4\tau_c^2}\left(t\exp\left(-\frac{t}{2\tau_c}\right)-\frac{4\tau_c^2}{\tau}\left(1-\exp\left(-\frac{t}{2\tau_c}\right)\left(1+\frac{t}{2\tau_c}\right)\right)\right) && \text{for } \zeta=1\end{aligned}$$

$$= \frac{\tau}{K}\frac{\Delta y_{sp}}{2\tau_c\zeta^2 x}\left(\exp\left(-\frac{t}{2\tau_c}\right)\sinh\left(\frac{x}{2\tau_c}t\right) - \frac{2\tau_c\zeta^2 x}{\tau}\right. \quad \text{(A12)}$$

$$\left.\left(1-\exp\left(-\frac{t}{2\tau_c}\right)\left(\cosh\left(\frac{x}{2\tau_c}t\right)+\frac{1}{x}\sinh\left(\frac{x}{2\tau_c}t\right)\right)\right)\right) \quad \text{for } \zeta>1$$

The steady-state response of the manipulated variable to a step change in the set point is defined as t approaches infinity:

$$u_{ss}(t\to\infty) = \frac{\Delta y_{sp}}{K} \quad \text{(A13)}$$

The peak of u(t) can be found from du(t)/dt=0 as

$$u_{ss}(t\to\infty) = \frac{\Delta y_{sp}}{K} \quad \text{(A14)}$$

$$t_{peak} = \frac{2\tau_c}{x}\tan^{-1}\left(\frac{2}{1-2\frac{\tau_c}{\tau}}\right) \quad \text{for } 0<\zeta<1$$

$$= \frac{2\tau_c}{1-2\frac{\tau_c}{\tau}} \quad \text{for } \zeta=1 \quad \text{(A15)}$$

$$= \frac{2\tau_c}{x}\tanh^{-1}\left(\frac{x}{1-2\frac{\tau_c}{\tau}}\right) \quad \text{for } \zeta>1$$

Therefore,

$$u_{peak} = \left|\frac{\tau}{K}\frac{\Delta y_{sp}}{\tau_c} f(\zeta,\tau_c)\right| \quad \text{(A16)}$$

where

$$f(\zeta,\tau_c) = \frac{\tau_c}{\tau} + \frac{\sqrt{\left(1-2\frac{\tau_c}{\tau}\right)^2 + x^2}}{2}\exp\left(-\frac{1}{x}\tan^{-1}\left(\frac{X}{1-2\frac{\tau_c}{\tau}}\right)\right) \quad \text{for } 0<\zeta<1$$

$$= \frac{\tau_c}{\tau} + \frac{1-2\frac{\tau_c}{\tau}}{2}\exp\left(-\frac{1}{1-2\frac{\tau_c}{\tau}}\right) \quad \text{for } \zeta=1 \quad \text{(A17)}$$

$$= \frac{\tau_c}{\tau} + \frac{\sqrt{\left(1-2\frac{\tau_c}{\tau}\right)^2 + x^2}}{2}\exp\left(-\frac{1}{x}\tanh^{-1}\left(\frac{X}{1-2\frac{\tau_c}{\tau}}\right)\right) \quad \text{for } \zeta>1$$

Thus, the constraint given in Eq. (4-4) can be expressed as follows in Eq. (A17):

$$\left|\frac{\tau}{K}\frac{\Delta y_{sp}}{\tau_c} f(\zeta,\tau_c)\right| \le u_{max} \quad \text{(A18)}$$

4. Appendix D: Derivation of the Constraint Given in Eq. (4-3)

The rate of change in the manipulated variable, u′(t), can be obtained by differentiating equation in Eq. (A12)

$$u'(t) = -\frac{\tau}{4K}\frac{\Delta y_{sp}}{\tau_c^2\zeta^2 x}\exp\left(-\frac{t}{2\tau_c}\right)\left(-x\cos\left(\frac{x}{2\tau_c}t\right)+\left(1-2\frac{\tau_c}{\tau}\right)\sin\left(\frac{x}{2\tau_c}t\right)\right)$$

$$\text{for } 0<\zeta<1$$

$$= -\frac{\tau}{4K}\frac{\Delta y_{sp}}{\tau_c^2}\exp\left(-\frac{t}{2\tau_c}\right)\left(-1+\frac{t}{2\tau_c}\left(1-2\frac{\tau_c}{\tau}\right)\right) \quad \text{for } \zeta=1 \quad \text{(A19)}$$

$$= -\frac{\tau}{4K}\frac{\Delta y_{sp}}{\tau_c\zeta^2 x}\exp\left(-\frac{t}{2\tau_c}\right)\left(-x\cos\left(\frac{x}{2\tau_c}t\right)+\left(1-2\frac{\tau_c}{\tau}\right)\sinh\left(\frac{x}{2\tau_c}t\right)\right)$$

$$\text{for } \zeta>1$$

The steady-state response of the rate of change in the manipulated variable to a step change in the set point is defined as t approaches infinity:

$$u'_{ss}(t\to\infty) = 0 \quad \text{(A20)}$$

The peak of u′(t) can be found from du′(t)/dt in terms of ζ and τ_c as:

$$u'_{peak} = \left|\frac{\tau}{K}\frac{\Delta y_{sp}}{\tau_c^2}\right| h(\zeta) \quad \text{(A21)}$$

where

$$h(\zeta) = \frac{1}{4\zeta^2} \quad \text{for } \zeta>0 \quad \text{(A22)}$$

Therefore, the constraint given by Eq. (4-4) can be expressed as:

$$\left|\frac{\tau}{K}\frac{\Delta y_{sp}}{\tau_c^2}\right| h(\zeta) \le u'_{max} \quad \text{(A23)}$$